A Statistical Study of the Application of Incoherent Integration to Simulated Equatorial Electrojet Irregularities Power Spectra

Henrique C. Aveiro* [1,2], Clezio M. Denardini [3], Mangalathayil A. Abdu [3], Nelson J. Schuch[1], Cleomar P. da Silva [1,2]

[1] Instituto Nacional de Pesquisas Espaciais – Centro Regional Sul de Pesquisas Espaciais – Santa Maria, RS, Brazil;
[2] Universidade Federal de Santa Maria – Laboratório de Ciências Espaciais de Santa Maria – Santa Maria, RS, Brazil;
[3] Instituto Nacional de Pesquisas Espaciais – Divisão de Aeronomia – São José dos Campos, SP, Brazil.

This paper was prepared for presentation at the 9th International Congress of the Brazilian Geophysical Society held in Salvador, Brazil, 11-14 September 2005.

Abstract

The RESCO 50 MHz coherent back-scatter radar has been operated since 1998 at the INPE/MCT's São Luís Space Observatory (2.33° S, 44.2° W, DIP: -0.5°), Brazil, on the dip equator to study the equatorial electrojet dynamics. Spectral analysis of the received echo from equatorial electrojet irregularities allow us to identify the dominant type of plasma irregularities in the electrojet bulk observed by the radar. Using curve fitting methods on the resulting power spectra it is also possible to obtain other characteristics from the echoes, such as: center of frequency distribution, spectral width and power. The usual approach in this analysis is through a Gaussian fitting based on the method of Least Square Error to parameters estimation. Before fitting the power spectra it is usual to smooth it in order to reduce the noise level and define better the center of frequency distribution. From the center of frequency distribution, we are able to deduce the Doppler shift of the irregularities in relation to the radar, which is close related to the electric fields that drives the plasma instabilities. In this work, we have simulated echoes signals from 3-meter type 1 plasma instabilities, and analyzed it in order to recover the center of frequency distribution used to simulate the data generated. As a smoothing method we have used incoherent integration. We have applied three distinct levels of smoothing in order to evaluate the response of the fitting to this technique. The advantages and disadvantages of applying different levels of incoherent integration over power spectra of back-scatter echoes from type 1 irregularities in the parameter estimation are presented and discussed.

Introduction

Between about 90 and 120 km of altitude (at the E region heights) and covering a latitudinal range of ±3º around the dip equator flows an intense electric current, denominated equatorial electrojet, EEJ (Forbes, 1981). It is driven by the E region dynamo (Fejer and Kelley, 1980) and it plays an important rule in the phenomenology control of the ionosphere-thermosphere system. The EEJ was initially detected in the first half of the twentieth century as geomagnetic large scale variations in magnetic observatories close to the equator. Egedal (1948) was the first one to conclude that this variation was due to an electric current flow under the magnetic dip equator; however, it was Chapman (1951) who first explained it, terming this phenomenon as equatorial electrojet.

Studies of the equatorial ionosphere using VHF radars have shown echoes back-scattered from electron density irregularities in the EEJ. These studies showed distinct spectral signature for the two types of irregularities, called type 1 and type 2, also known as two-stream (Farley, 1963; Buneman, 1963) and gradient drift, respectively. Several experiments have been done to investigate the EEJ irregularities in order to characterize its spectra and explain the phenomenology (Bowles et al., 1963; Bowles and Cohen, 1962; Cohen and Bowles, 1967; Balsley, 1969; Gupta and Krishna Murthy, 1975; Hanuise et al., 1979; Crochet et al., 1979).

In 1998, the RESCO 50 MHz coherent back-scatter radar entered in operation at the INPE/MCT's São Luís Space Observatory, Brazil, on the magnetic equator. Since then several studies have been conduced in the Brazilian sector (Abdu et al. 2002, 2003; Denardini et al., 2004). Through the constant monitoring of the EEJ irregularities, we can have a radiography of E region electric fields (Schieldge et al., 1973, Farley and Fejer, 1975; Reddy, 1981; Reddy and Devasia, 1981; Viswanathan et al., 1987; Reddy et al., 1987; Hysell et al., 1997; Hysell and Burcham, 2000; Denardini, 2003). In this context, the correct estimation of the Doppler shift from the irregularities echoes power spectra is a crucial point. And the curve fitting is presented as an efficient toll to determine the irregularities Doppler shift (Kudeki et al., 1999; Denardini, 2004). The curve fitting as a parameter estimation technique is based on finding the parameters of a well known mathematic equation, trying to minimize the mean square errors between observational data and the fit curve (Levenberg, 1944; Marquardt, 1963).

It is known that the incoherent integration reduces the signal variance (Fukao, 1989). In order to improve the techniques of RESCO radar data analysis, we have study the incoherent integration technique applied to power spectra of simulated back-scatter signals from type 1 irregularities from EEJ. This statistical study aimed to quantify the advantages and disadvantages of applying such technique. The methodology of this work as well as the results is discussed in details.

Theory and Method

The RESCO coherent back-scatter radar is operated routinely during two weeks per month. It is usually set for EEJ sounding transmitting one pulse each 1-2 ms with pulse width of 20 μs and time delay of 600 μs. Therefore, the power spectra within the Doppler frequencies, related to the Doppler shift, obtained from Fast Fourier Transform (FFT), have an aliasing frequency of 250-500 Hz. The frequency resolution is determined by the number of subsequent pulses taken for the FFT analysis and by the aliasing frequency.

From each spectrum, seven parameters are estimated through curve fitting. We usually fit the sum of two Gaussian curves to the spectrum, each one related to one type of irregularity.

Once the focus of the work is the study of type 1 irregularity spectra, the Gaussian covariance model of Zrnic (1979) was used to simulate power spectra of 3-meters plasma irregularities containing only the characteristics of the Farley-Buneman instability. Type 1 power spectra were simulated having 256 points each one. All these spectra were chosen to have f_d = 120 Hz, σ=20 Hz, P_N=0.5 W and signal-to-noise ratio (SNR) equals to 3 dB. The white noise was added to the data in time domain in order to assure a more realistic variance in the power spectra. So, each spectrum simulated is described by a noise level added to a Gaussian curve (Takeda et al., 2001), i.e., our data set was described by one function S in relation to the frequency f, given by:

$$S(f) = \frac{P}{\sigma\sqrt{2\pi}} \exp\left[-\frac{(f - f_d)^2}{2\sigma^2}\right] + P_N \quad , \qquad (1)$$

where P, f_d, σ and P_N are, respectively, the spectral power, the center of frequency distribution (corresponding to Doppler shift), spectral width and noise level. An example of a spectrum simulated is presented in Figure 1 where the quantities mentioned above are indicated in different colors. The green dashed line represents the noise power density (P_N), the vertical red line shows the center of frequency distribution (f_d), the difference between the vertical orange and red lines determines the standard deviation of the curve fitted to the power spectrum and the area between the blue dashed line and the green dashed line defines the power of the signal (P).

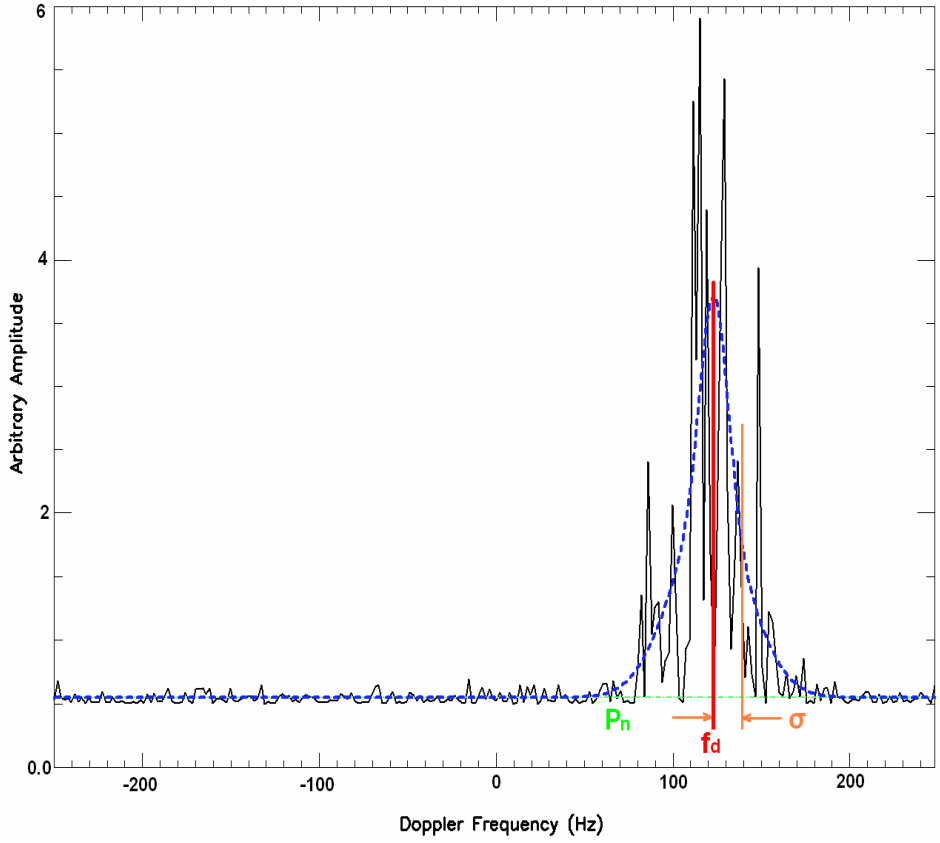

Figure 1 – Power spectrum simulated (black line) superimposed by a Gaussian curve (blue line) fitted to the spectrum using Least Square Error Method. The green dashed line represents the noise power density (P_N), the vertical red line shows the center of frequency distribution (f_d), the difference between the vertical orange and red lines determines the standard deviation of the Gaussian curve fitted to the spectrum and the area between the blue dashed line and the green dashed line defines the power of the signal (P).

We started step two analyzing the simulated power spectra after having a proper data set with *a priori* type 1 characteristics from which we could establish comparison with the parameters estimated by the method. To reduce our data set of 256 points to 4 parameters, we have used the Maximum Likelihood Estimation with the purpose of minimize the square sum of residual error as given by (Woodman, 1985):

$$\varepsilon^2 = \sum_{i=1}^{N} [y_i - S(f_i; P, f_d, \sigma)]^2 \quad , \qquad (2)$$

where N is the number of frequency points and y_i is the observed spectral amplitude for one given frequency.

Curve fitting algorithms usually give not good result when the data variance is high. To attempt reducing the variance, we usually integrate incoherently consecutive spectra, i.e., we smooth the spectra. Once the noise is a random component, the resultant spectrum will tend to have minor variance. An illustration of incoherent integration applied to hundred consecutive spectra like the first on the left side, with the resulting mean spectra aside is presented in Figure 2. In this illustration we see a noise bunch of spectra (represented by the first one) on the left side transformed into a smoothed one on the right side.

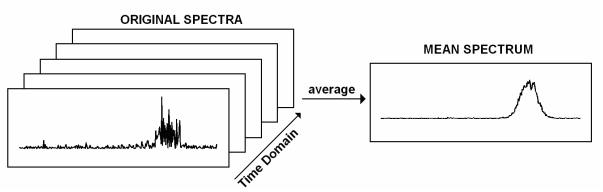

Figure 2 – Illustration of incoherent integration applied to hundred consecutive spectra like the first on the left side.

The detectability of a Doppler spectrum can be defined as per (Gage and Balsley, 1978):

$$D \equiv \frac{P_S}{\sigma_N} \quad , \qquad (3)$$

where P_S is the peak spectral density of the power spectrum and σ_N is the standard deviation of noise. The noise power density has a chi-squared distribution with 2 degrees of freedom, since P_N results from the squared sum of real and imaginary components of the amplitude spectrum. The application of incoherent integration, by averaging the N_i consecutive spectra, does not changes the mean values of spectral densities of signal and noise. The effect of incoherent integration is just increasing the degrees of freedom of the chi-squared distribution, instead of 2 degrees with no integration, it would have $2xN_i$ degrees of freedom, increasing too the detectability by $\sqrt{N_i}$ (Fukao, 1989). For this reason the Gaussian curve becomes more visible in Figure 2.

Results

It was generated 10,000 simulated power spectra within type 1 irregularity characteristics, such as f_d = 120 Hz. Afterwards, we have integrated incoherently every group of 10 and 100 spectra, in order to created two other data set. So, we have three groups of spectra were the first one have 10,000 spectra not smoothed, the second one have 1,000 spectra smoothed by 10 incoherent integrations, and the third one having 100 spectra smoothed by 100 incoherent integrations.

Every spectrum of the three groups was fitted by a single Gaussian to analyze the result of the fitting using Least Square Error. After estimating the spectral moments of the individual curves, we analyze the answer of the method in the determination of f_d in relation to the *a priori* f_d values used to generate the power spectra with type 1 characteristics. As a result of our analysis, we present in Figure 3 the histograms of the Doppler frequencies estimated from the simulated data. Each bar is centered in the integer frequency defined in the Y axis with ± 0.5 Hz of resolution. The red bar shows the locus of f_d = 120 ± 0.5 Hz used to simulate the spectra, and, hence, the expected answer. The histogram of Figure 3-a shows the distribution of the answer of fitting method to the case with no incoherent integration applied to the spectra. The histogram of the Figure 3-b shows the distribution of the answer of fitting method to the case were incoherent integration of 10 spectra was applied. And the histogram of 3-c shows the distribution of the answer of fitting method to the case were incoherent integration of 100 spectra was applied. One should remember, however, that the number of answer is different for the different histograms in Figure 3. For the histogram 3-a, we have 10,000 answers while for 3-b we have 1,000 and 100 for the 3-c. Nevertheless, the number of samples used do not imply in drastic changes in the results. We expect the same confidence limit in results with different number of samples.

The Figure 3 reveals the higher the number of incoherent integration the higher the number of answers close to the right value. A clear interpretation of this result is to assume that, as we increase the number of spectra in the incoherent integration, we improve the number of success in estimating the test parameter (f_d). However, the application of the technique implies in increasing time resolution. In the case of incoherent integration of 10 spectra, the time resolution is increased by 10, i.e., our resolution suffers an increase directly proportional to the number of spectra used in the integration.

Quantitatively, using no incoherent integration, 9.25% of the answer where close to the *a priori* f_d value. Using incoherent integration of 10 spectra, 54.40% of the answer where close to the *a priori* f_d value. And, using incoherent integration of 100 spectra, 99.00% of the answer where close to the *a priori* f_d value. This indicated that the efficiency of the method was increased from 9.5% to 99.0%, with a statistical error of 0.42% (± 0.5 Hz), when we go from no use of incoherent integration to the use of incoherent integration of 100 spectra. In this case, the degrees of freedom of P_N were increased from 2 to 200 and the detectability of the Doppler spectrum was increased by 10. In the same way, using 10 spectra, the degrees of freedom of P_N were increased from 2 to 20 and the detectability of the Doppler spectrum was increased by 3.16.

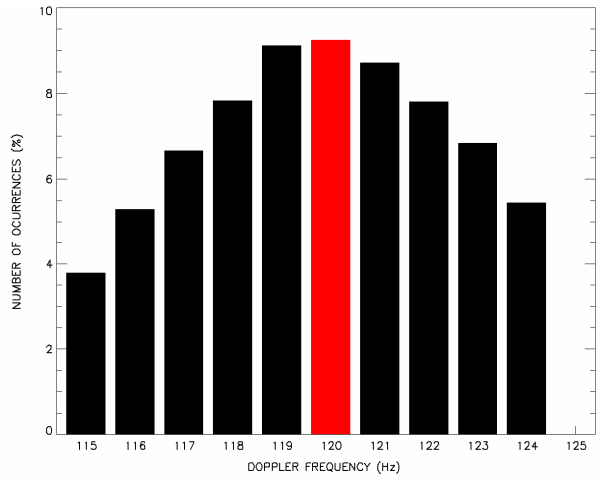

(a)

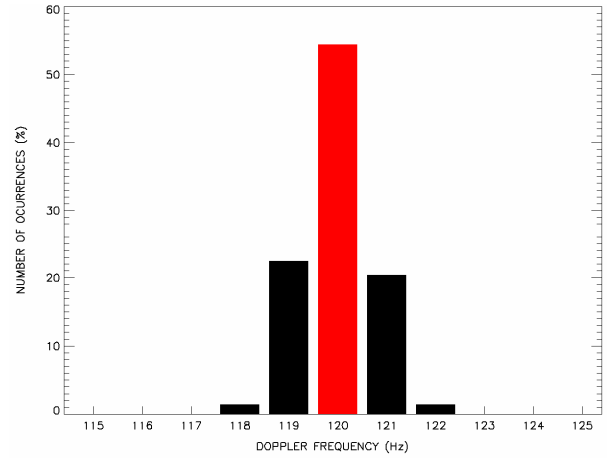

(b)

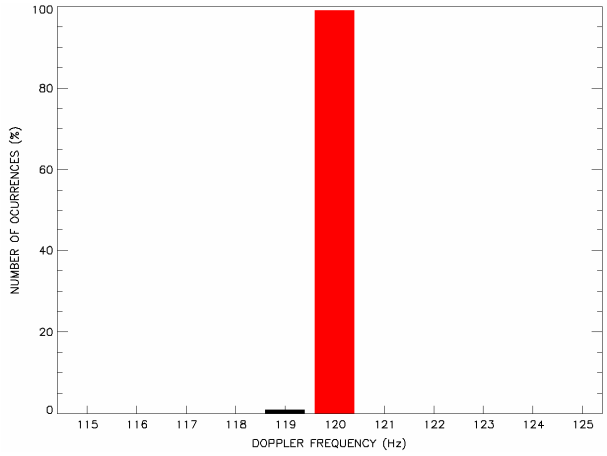

(c)

Figure 3 – Histograms of Central Frequency estimated by Least Square Error using spectra with no incoherent integration (3.a), integration of 10 spectra (3.b) and integration of 100 spectra (3.c). In the figures, the red bars mean the expected result of the estimation, f_d =120 ± 0.5 Hz.

Conclusions

The technique of incoherent integration showed itself a valuable tool with significant improvement in the determination of the test parameter, the center of the frequency distribution (f_d) of the EEJ irregularities power spectra. Increasing the number of incoherently integrated spectra, we can improve the parameters estimation; however, we have depreciation of the time resolution. In the case of the RESCO radar, where we normally have one spectrum per 6 seconds, integrate incoherently 10 spectra would mean to increase the resolution to one spectrum per minute. For EEJ dynamics studies this number of integrations would not compromise the analysis. However, despite a high number of integrated spectra would improve considerably the estimation of the center of frequency distribution, as we have shown in the present study, it could lead to an undesirable time resolution. This could compromise future analyses of correlation, as between the RESCO radar data and auroral indices, for example.

Acknowledgments

H. C. A. and C. P. S. wish to thank CNPq/MCT for financial support to their undergraduate programs through the projects nr. 107616/2003-3 and 104427/2004-3, respectively.

References

Abdu, M. A., Denardini, C. M., Sobral, J. H. A., Batista, I. S., Muralikrishna, P. and de Paula, E. R., 2002, Equatorial electrojet irregularities investigations using a 50 MHz back-scatter radar and a Digisonde at São Luís: Some initial results: Journal of Atmospheric and Solar-Terrestrial Physics, Vol. 64, No. 12-14, p.1425-1434.

Abdu, M. A., Denardini, C. M., Sobral, J. H. A., Batista, I. S., Muralikrishna P., Iyer, K. N., Veliz, O. and de Paula, E. R., 2003, Equatorial electrojet 3 m irregularity dynamics during magnetic disturbances over Brazil: results from the new VHF radar at São Luís: Journal of Atmospheric and Solar-Terrestrial Physics, Vol. 65, No. 14-15, p.1293-1308.

Balsley, B. B., 1969. Some characteristics of non-two-stream irregularities in the equatorial electrojet: Journal of Geophysical Research, Vol. 74, p.2333-2347.

Bowles, K. L. and Cohen, R., 1962. A study of radio wave scattering from sporadic E near the magnetic equator, in *Ionospheric Sporadic E*, edited by E. K. Smith and S. Matsushita, Pergamon, New York.

Bowles, K. L., Balsley, B. B. and Cohen, R., 1963. Field-aligned E region irregularities identified with ion acoustic waves: Journal of Geophysical Research, Vol. 68, p.2485-2497.

Buneman, O., 1963. Excitation of field aligned sound waves by electron streams: Physical Review Letters, Vol. 10, No. 7, p.285-287.

Chapman, S., 1948, The abnormal daily variation of horizontal force at Huancayo and Uganda: Journal of Geophysical Research, Vol. 53, p.247-250.

Chapman, S., 1951, The equatorial electrojet as detected from the abnormal electric current distribution about Huancayo, Peru and elsewhere: Archives Fur Meteorology, Geophysics and Bioclimatologie, A44, p.368-390.

Cohen, R. and Bowles, K. L., 1967. Secondary irregularities in the equatorial electrojet: Journal of Geophysical Research, Vol. 72, p.885-894.

Crochet, M., Hanuise, C. and Broche, P., 1979, HF radar studies of two-stream instability during a equatorial counter-electrojet: Journal of Geophysical Research, Vol. 84, p.5223-5233.

Denardini, C. M., 2003, Estudo da eletrodinâmica da ionosfera equatorial durante o período de máxima atividade solar (1999-2002): São José dos Campos, Instituto Nacional de Pesquisas Espaciais, Thesis.

Denardini, C. M., 2004, Estimação de parâmetros de dados físicos: São José dos Campos, Instituto Nacional de Pesquisas Espaciais.

Denardini, C. M., Abdu, M. A. and Sobral, J. H. A., 2004, VHF radar studies of the equatorial electrojet 3-m irregularities over São Luís: day-to-day variabilities under auroral activity and quiet conditions: Journal of Atmospheric and Solar-Terrestrial Physics, Vol. 66, n17, p.1603-1613.

Egedal, J., 1948, Daily variation of the horizontal magnetic force at the magnetic equator: Nature, Vol. 161, p.443-444.

Farley, D. T., 1963, A plasma instability resulting in field aligned irregularities in the ionosphere: Journal of Geophysical Research, Vol. 68, No. A22, p.6083-6097.

Farley, D. T. and Fejer, B. G., 1975, The effect of the Gradient Drift term on type 1 electrojet irregularities: Journal of Geophysical Research, Vol. 80, No. A22, p.3087-3090.

Fejer, B. G. and Kelley, M. C., 1980, Ionospheric Irregularities: Reviews of Geophysics and Space Physics, Vol. 18, No. 2, p.401-454.

Forbes, J. M., 1981, The Equatorial Electrojet: Reviews of Geophysics and Space Physics, Vol. 19, No. 3, p.469-504.

Fukao, S., 1989, Middle atmosphere program – Handbook for map: International school on atmospheric radar, Vol. 30, Urbana (IL): SCOSTEP Secretariat.

Gage, K. S. and Balsley, 1978, Doppler radar probing of the clear atmosphere: Bulletin of American Meteorological Society, Vol. 59, p.1074-1093.

Gupta, K. S. and Krishna Murthy, B. V., 1975, On the sudden disappearance of equatorial sporadic E: Journal of Geomagnetism and Geoelectricity, Vol. 27, p.131-138.

Hanuise, C., Crochet, M., Gouin, P. and Ogubazghi, G., 1979, Radar observation of the equatorial counter-electrojet: Annales Geophysicae, Vol. 35, p.201-202.

Hysell, D. L. and Burcham, J. D., 2000, Ionospheric electric field estimates from radar observations of the equatorial electrojet: Journal of Geophysical Research, Vol. 105, No. A2, p.2443-2460.

Hysell, D. L., Larsen, M. F. and Woodman, R. F., 1997, JULIA radar studies of the electric field in the equatorial electrojet: Geophysical Research Letters, Vol. 24, No. 13, p.1687-1690.

Kudeki, E., Bhattacharyya, S. and Woodman, R. F., 1999, A new approach in incoherent scatter F region E x B drift measurements at Jicamarca: Journal of Geophysical Research, Vol. 104, No. A12, p.28145-28162.

Levenberg, K., 1944, A method for the solution of certain non-linear problem in least square: Quarterly Applied Mathematics, Vol. 2, No. 1, p.164-168.

Marquardt, D. W., 1963, An algorithm for least square estimation of non linear parameters: Journal of the Society for Industrial and Applied Mathematics, Vol. 2, No. 2, p.431-441.

Reddy, C. A., 1981, The equatorial electrojet: a review of ionospheric and geomagnetic aspects: Journal of Atmospheric and Terrestrial Physics, Vol. 43, No. 5/6, p.557-571.

Reddy, C. A. and Devasia, C. V., 1981, Height and latitude structure of the electric fields and currents due to local East-West winds in the equatorial electrojet: Journal of Geophysical Research, Vol. 86, No. A7, p.5751-5767.

Reddy, C. A., Vikramkumar, B. T. and Viswanathan, K. S., 1987, Electric fields and currents in the equatorial electrojet deduced from VHF radar observations – I. A method of estimating electric fields: Journal of Atmospheric and Terrestrial Physics, Vol. 49, No. 2, p.183-191.

Schieldge, J. P., Venkateswaran, S. V. and Richmond, A. D., 1973, Ionospheric dynamo and equatorial magnetic variations: Journal of Atmospheric and Terrestrial Physics, Vol. 35, No. 6, p.1045-1061.

Takeda, S., Nakamura, T. and Tsuda, T., 2001, An improvement of wind velocity estimation from radar Doppler spectra in the upper mesosphere: Annales Geophysicae, Vol. 19, p.837-844.

Viswanathan, K. S., Vikramkumar, B. T. and Reddy, C. A., 1987, Electric fields and currents in the equatorial electrojet deduced from VHF radar observations – II. Characteristics of electric fields on quiet and disturbed days: Journal of Atmospheric and Terrestrial Physics, Vol. 49, No. 2, p.193-200.

Woodman, R. F., 2001, Spectral moment estimation in MST radars: Radio Science, Vol. 20, No. 6, p.1185-1195.

Zrnic, D. S., 1979, Estimation of spectral moments of weather echoes: IEEE Transactions of Geoscience on Electronics, Vol. 17, p.113-128.